HEAT TRANSFER AT THE PHASE INTERFACE OF CONDENSING BUBBLES

F. Mayinger and Y. M. Chen

Lehrstuhl A für Thermodynamik, Technische Universität München, West Germany
National Taiwan University, Taipei, Taiwan

ABSTRACT

Using the holographic interferometry and the high speed cinematography heat transfer at the phase interface of vapour bubbles condensing in subcooled liquid of the same substance was measured with ethanol, propanol, refrigerant R 113 and water. The holographic interferometry gave also information on the boundary layer conditions at the liquid side, representing the main heat transfer barrier.
The measurements were performed in the range $2 < Pr < 15$ and $1 < Ja < 120$. Measured data could be well correlated as functions of Prandtl- and Reynolds-number for heat transfer and of Archimedes-, Prandtl- and Jacob-number for bubble collapse time.

1. INTRODUCTION

The thermo- and hydrodynamic phenomena during the collapse of vapour bubbles in liquids having a temperature below saturation conditions - so called subcooled liquids - are of technical and scientific interest for a better understanding of the instability condition in two-phase flow with subcooled boiling and in cavitation. The temporal course of the collapse of a vapour bubble during condensation in a subcooled liquid can be controlled by two different phenomena:

- The heat transfer at the phase interface of vapour and liquid and
- the inertia of the liquid mass when entering into the space set free by the condensing vapour.

With moderate temperatur differences between vapour and subcooled liquid the heat transport will be the governing process for the volumetric decrease of the bubble. This heat transfer process at the phase interface is influenced by the thermo-physical properties like heat conductivity, specific heat, latent heat of evaporation, density, viscosity and surface tension. Also the gradient of the saturation line plays a role. The thermophysical properties can be expressed in dimensionless numbers like the Prandtl-number

$$Pr = \frac{\eta_F \, c_P}{\lambda_F} \qquad (1)$$

and the Jacob-number

$$Ja = \frac{\varrho_F \, c_P \, (T_S - T_\infty)}{\varrho_D \, \Delta h_{FD}} \qquad (2)$$

With bubbles moving in the liquid also the Reynolds-number

$$Re = \frac{2 R w \varrho_F}{\eta_F} \qquad (3)$$

has to be taken in account with the relative velocity w_{rel} between the bubble and the liquid and the radius of the bubble as characteristic parameters. Finally the Fourier-number

$$Fo = \frac{a_F \, t}{(2R)^2} \qquad (4)$$

can be used as a dimensionless time for describing the duration of the collapsing period.

There is a large number of theoretical and experimental studies in the literatur dealing with condensation of bubbles. An extensive and comprehensive discussion of the status of art can be found for example in the papers by Hammitt /1/ and Theofanous /2/. In the case of inertia controlled condensation Plesset /3/ and Hammitt /4/ found good agreement with Rayligh's correlation /5/ developed beginning of this century. The situation with heat transport controlled condensation seems more complicated. Various authors describe the heat transfer at the phase interface of a condensing bubble similar to that around a moving solid sphere /6,7/ or a liquid droplet /8/. Examples of equations describing the bubble collapse are presented in Tab. 1. The equations

Author	Equation	Remarks
Florschuetz and Chao /9/	$\beta = \frac{R}{R_0} = 1 - \sqrt{\tau_H}$	$\tau_H = \frac{16}{\pi} \cdot Ja^2 \cdot Fo$
Voloshko and Vurgaft /10/	$\beta = 1 - 6{,}776 \cdot 10^{-1} \cdot Fo$	experimental $40 < Ja < 75$
Voloshko, Vurgaft and Aksel rod /8/	$\beta = \left[1 - \frac{6 - K}{\sqrt{\pi}} \cdot Ja \cdot Pe^{1/2} \cdot Fo\right]^{1/3}$	with $K = 1{,}88$ from experiment
Mealem and Sideman /6/	$\beta = \left[1 - \frac{3}{\sqrt{\pi}} \cdot Ja \cdot Pe^{1/2} \cdot Fo\right]^{2/3}$ $\beta = \left[1 - \frac{5}{2} \cdot \frac{1}{\sqrt{\pi}} \cdot Ja \, Pe^{1/2} \cdot Fo\right]^{1/5}$	for $2 < R_0 < 4\,mm$ for $R_0 < 1\,mm$
Akiyama /7/	$\beta = \left[1 - 2{,}8 \cdot C \cdot Pr^{-0{,}27} \cdot Ja \cdot Pe^{0{,}4} \cdot Fo\right]^{1/3}$	with $C = 0{,}27$
Dimic /11/	$\beta = \left[1 - 5 \frac{1}{\sqrt{\pi}} (3 \cdot \zeta)^{-1/2} \cdot Ar^{1/4} \cdot Pr^{1/2} \cdot Ja \cdot Fo\right]^{1/5}$ $\beta = \left[1 - 7 \left(\frac{2{,}7}{\pi}\right)^{1/2} \cdot K_g^{1/4} \cdot Ja \cdot Fo\right]^{1/7}$	for $Re > 31 \, K_g^{0{,}25}$ with $\zeta = 2{,}61$ for $4{,}02 \cdot K_g^{0{,}25} < Re < 31 \cdot K_g^{0{,}25}$

Tab.1 : Some equations predicting the heat transport at condensing bubbles

there can be reduced to the simple form

$$\beta = \frac{R}{R_0} = [1 - K \, Ja \, Fo] \qquad (5)$$

where β is the ratio of the momentary radius R of the bubble to its initial one (R_0) and where the factor K represents a constant or a function describing the heat transfer at the phase interface. Besides the Jacob-, Fourier-, and Prandtl-number also the Peclet-number

$$Pe = \frac{2 R_0 w_0}{a_F} \qquad (6)$$

and the Archimedes-number

$$Ar = \frac{g (2 R_0)^3}{\nu_F^2} \qquad (7)$$

are used in some of these equations. Dimić /11/introduces an additional dimensionless variable K_σ

$$K_\sigma = \frac{R_0 \sigma}{\rho_F a_F^2} \qquad (8)$$

describing the influence of the surface tension. The agreement of data predicted with these equations is not too good, which maybe mainly due to the unknown heat transfer conditions. Nordmann and Mayinger /12/therefore used the holographic interferometry to get a better insight into the thermo- and fluiddynamic behaviour at the phase interface and by this to gain information on the heat transport conditions. The research activities and results reported here are a continuation of this work /12/.

2. EXPERIMENTAL TECHNIQUE

In the literature the following techniques are reported for generating bubbles in a subcooled liquid:

- Superheating of a liquid boundary layer on a heated surface
- blowing saturated vapour through a nozzle into subcooled liquid
- flashing by depressurization
- local heating by a focused Laser-beam.

To guarantee the boundary conditions as simple and as homogeneous as possible in the experiments reported here the bubbles were produced by blowing saturated vapour through a nozzle, shown in figure 1, into a subcooled liquid moving slowly downward.

The vapour needed for generating the bubbles flows through the channel in the center to the small chamber being situated at the inner end of the nozzle. The nozzle consists of a short capillary having a diameter of 1,6 mm. This capillary diameter was found as a compromise because a too large diameter influences the size and the shape of the departing bubbles, and with a too small diameter the vapour flow could not follow the dynamic situation during generation and detachment of the bubbles. Around this central channel vapour is flowing in an annulus acting as guardheater guaranteeing that the vapour for generating the bubbles is exactly saturated. Before starting the bubble formation the capillary is closed at its inner end by a needle to avoid that liquid enters the nozzle.

The liquid in which the bubble is forming and collapsing was extremely carefully degased and then cooled to a temperature temporally and locally as constant and homogeneous as possible. The latent heat of evaporation of the condensing vapour in the bubble is raising the temperature of the liquid. Therefore to guarantee that each bubble finds the same and equally

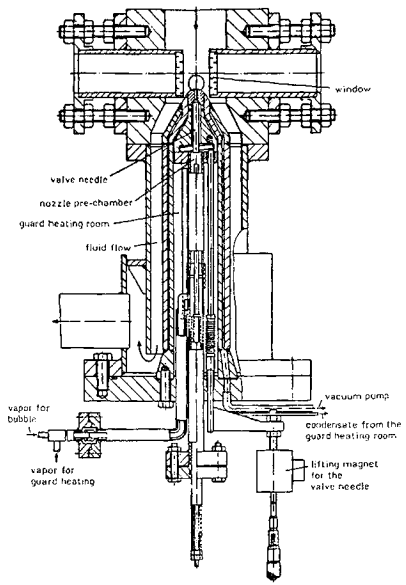

Fig.1 : Test section

subcooled temperature field the liquid flows with a velocity of approximately 2 cm/s downwards against the nozzle. This small velocity does not influence the detachment and the raising velocity of the bubble.

As mentioned above the heat transfer at the phase interface was investigated by the holographic interferometry in connection with the high speed cinematography. The arrangement of the used optical set-up is schematicalaly shown in figure 2. Due to the small diameter of the bubble, the strong curvature of the phase interface, together with the high temperature gradient in the boundary layer on the liquid side the methods known in the literature - e.g. Abel-integral - are not sufficient to analyse and evaluate the interferograms. The deflection of the beam passing through the temperature field around the bubbles is not negligible as assumed with the Abel correction. Therefore the following correction procedure was developed.

A first analysis of the interferogram is performed without regarding the deflection of the light beam. With the equation

$$\varepsilon(y)\,\lambda_0 = \int_{-z_\infty}^{z_\infty} [n(r) - n_\infty]\, dz \qquad r_B \le y \qquad (9)$$

the phase shift between the measuring and the reference waves figure 2 is calculated by means of the order of the fringes $\varepsilon(y)$ and the wave length λ_0 of the applied light. The deflection of a beam travelling through the liquid boundary layer around a condensing vapour bubble is schematically shown in figure 3. Due

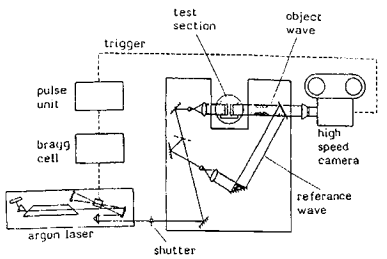

Fig.2 : Holographic interferometer

to the continously changing temperature in the boundary layer and the resulting change of the refractive index this beam has a curved trajectory. For an observer beyond the image plan it seems to come from the projected point F on the focussing plan. In the image plan (not shown in figure 3) the object beam interferes with the reference beam which was not

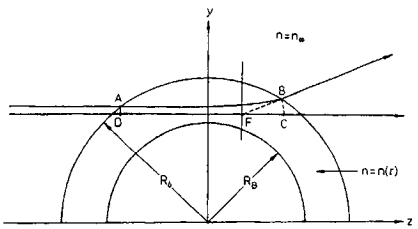

Fig.3 : Ligth beam trajectories with deflection

deflected. Both beams - object beam and reference beam - have the same phase relationship up to the points A and D. Assuming lenses of optical quality the optical path length of the two beams behind the points B and C to the image plan is equal. Therefore the interference only originates from the optical phase shift difference of the object beam running through the boundary layer of the bubble

$$\varepsilon(y)\,\lambda_0 = \int_A^B n\,ds - n_\infty \overline{DC} \qquad (10)$$

The path of the beam in the boundary layer is described by the following differential equation

$$\ddot{y} = \frac{1}{n}\,(1+\dot{y}^2)\left(\frac{\partial n}{\partial y} - \dot{y}\,\frac{\partial n}{\partial z}\right) \qquad (11)$$

where dots refer to the differentiation with respect to z.

From the equations (10) and (3) a new distribution of the interference fringes ε(y) can then be numerically evaluated. The refractive index field can now be easily converted into a temperature field if the dependence of the refractive index on the temperature dn/dT is known which was the case for all substances used in these experiments. The heat transfer coefficient can then be calculated with the well known equation

$$h = \frac{-k\left(\frac{\partial T}{\partial y}\right)_w}{T_w - T_\infty} \qquad (12)$$

assuming that a thin laminar boundary layer exists on the liquid side of the phase interface. Callibration tests of forced convection around a heated solid sphere were made to check the correction procedure mentioned above.

Measurements were performed with the substances
- refrigerant R 113
- Ethanol
- Propanol
- and in some cases with water.

The water measurements were only performed to demonstrate the agreement with former experiments /12/. Using these substances the Prandtl-number could be varied between 1,9 and 15.

With this holographic technique boundary layers down to 0,05 mm could be investigated with an accuracy high enough to predict the local heat transfer coefficient within ± 20%. In cases of still thinner boundary layers or with turbulent fluiddynamic conditions around the phase interface the heat transfer coefficient was evaluated from the temporal decrease of the bubble volume via an energy balance. This temporal decrease was measured with the high speed cinematography.

3. INTERFEROGRAMS AND THERMAL BOUNDARY LAYER AROUND CONDENSING BUBBLES

The situation in the boundary layer varies considerably during bubble formation and bubble detachment and is quite different at the bubble top and the bubble root as figure 4 for the substance Propanol demonstrates. Figure 5 shows the temporal course of the heat transfer - in terms of the Nusselt-number at the top and the equator of the bubble -evaluated from the interferograms of figure 4. In the first milliseconds the bubble is slowly growing by vapour adition out of the nozzle and the heat transfer is almost constant during this period (up to 60 ms). In the moment when the detachment of the bubble starts, which can be seen

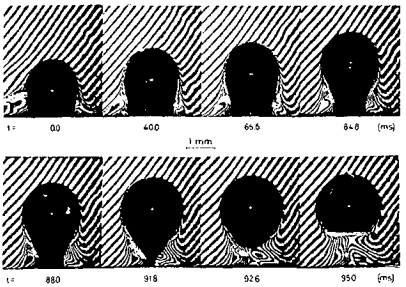

Fig.4 : Interferograms of a condensing propanol bubble (p = 2 bar, ΔT = 7.6 K, Ja = 7.1)

from the preceeding laceing of the bubble root, the heat transfer is increasing. When the bubble begins to move upward the boundary layer becomes considerably thinner at the upper surface of the bubble. The lower end of the bubble shows small oscillations producing a high turbulent vorteces in the drift flow.

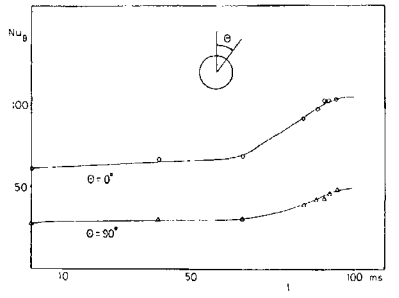

Fig.5 : Temporal course of the Nusselt number of the bubble shown in fig.4 (evaluated from interferograms in fig.4)

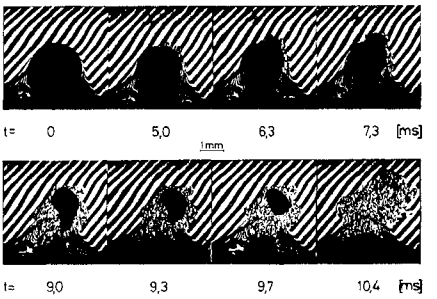

Fig.6 : Interferograms of a ethanol bubble with turbulent boundary layer
(p = 0.25 bar, ΔT = 20.6 K, Ja = 101.2)

With high Jacob-numbers, which correspond to a much higher subcooling, the situation around the bubble is completely different as figure 6 demonstrates. The phase interface becomes very early unstable due to local condensation effects and no laminar boundary layer can be observed around the bubble which condenses completely within a very short period of approximately 10 ms. Under these conditions the inertia of the liquid governs the bubble collapse.

The influence of the liquid Prandtl-number on to the boundary layer situation demonstrates figure 7 where interferograms of different substances but for approximately equal values of Reynolds- and Jacob-numbers are compaired. In this figure also data for the Nusselt-number and the heat transfer coefficient measured at the equator of the bubbles are shown. The

	Water	R113	Ethanol	Propanol
Re	= 250	300	290	320
Pr	= 1.97	5.7	9.0	14.4
Nu_{90}	= 29	41	52	63
h	= 5280 W/m²K	1430	2930	3470

Fig.7 : Comparison of boundary layer conditions with various Prandtl-numbers

Nusselt-number shows higher values with increasing Prandtl-number, however, regarding the heat transfer coefficient h the picture changes because the bubble diameter is used as characteristic length in the Nusselt-number and due to its higher surface tension water bubbles grow to a larger diameter until detaching than the bubbles of hydro-carbon substances. Also the thermal conductivity of water is by a factor of 5 to 10 higher than that of the other substances.

4. RESULTS AND EMPIRICAL CORRELATIONS

The holographic interferograms showed at least at the top of the bubble an influence of the relative velocity between bubble and liquid onto the heat transfer coefficient h or the Nusselt-number Nu respectively similar to that of a solid sphere under crossflow conditions. Therefore it was obvious to make a first trial for correlating the heat transfer by using the well known equation

$$Nu = 2 + C\ Re^m\ Pr^n \qquad (13)$$

which is valid for Reynolds-numbers between 0 and 200. In our experiments the Reynolds-numbers were always above 100 and reach up to 1000. Therefore pure conduction expressed by the 2 in equation (13) is of negligible influence on the result and equation 13 was simplified into the form

$$Nu = C\ Re^m\ Pr^n \qquad (14)$$

Using the bubble diameter at the moment of detachment as characteristic length in the Nusselt- and Reynolds-number and by carefully averaging the measured results the correlation

$$Nu = 0.185\ Re^{0.7}\ Pr^{0.5} \qquad (15)$$

was found for describing the mean heat transfer coefficient during the period when the bubble is still connected with the nozzle, i.e. before bubble detachment. This equation is experimentally verified for Reynolds-numbers between 100 and 1000, Prandtl-numbers between 6 and 20 and Jacob-numbers between 5 and 40. The equation is based on the assumption that the heat transport resistance is only on the liquid side which is certainly true for pure vapour not containing non condensible gases. Different from the conditions around a solid sphere the velocity at the phase

interface of a bubble is not zero and therefore the exponent with the Prandtl-number in equation (15) is higher than that for solid spheres.

A comparison between experimental data measured by the holographic interferometry and the predictions of equation (15) are shown in figure 8. The heat transfer at the surface of a bubble sticking at a nozzle but exposed to a slow crossflow is higher than that around a solid sphere which can be explained by the smaller shear stress at the phase interface and by the movability of the bubble surface.

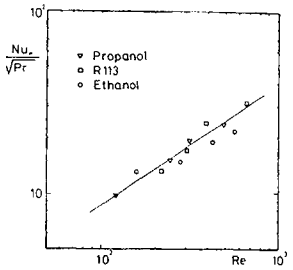

Fig.8 : Comparison of experimental data (holographic interferometry) with empirical correlation (eq.15)

With rising bubbles, i.e. after detachment, the heat transfer conditions become more complicated. As expected the high speed cinematography showed that the bubbles reach constant equilibrium velocity shortly after detaching from the nozzle. Therefore the attempt was made to describe the heat transfer around rising bubbles with the same form of the correlation as that for a sticking bubble. The question, however, is which characteristic length should be used in the Nusselt- and Reynolds-number. Due to condensation the bubble diameter decreases continuously while the bubble is rising. Using the instantaneous bubble diameter would need a rather extensive and iterative procedure for calculating the heat transfer. In the literature, however, reliable equations can be found for correlating the bubble diameter in the moment of bubble detachment. Therefore and with respect to a simpler procedure in practical use the bubble diameter at the moment of detachment was used which can be easily predicted by equation (16)

$$d = \sqrt[3]{\frac{6\,\sigma\,d_{Dü}}{\Delta\varrho\,g}} \qquad (16)$$

With the least square method the experimental results could be correlated in the simple form

$$Nu = 0.6\ Re^{0.6}\ Pr^{0.5} \qquad (17)$$

representing now data up to Reynolds-numbers of 10^4. The low value 0,185 of the constant in equation (17) is because of using the detachment diameter as characteristic length.

As shown in figure 9 these correlation corresponds well with measured data of different substances and of different origin. The correlation can be used up to a Jacob-number of approximately 80, as long as inertia effects do not play a dominant role.

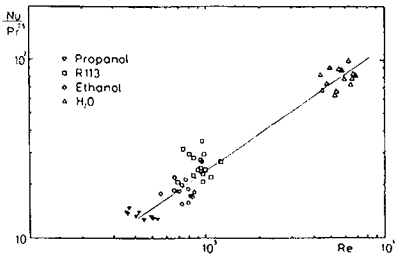

Fig.9 : Mean Nusselt numbers of rising bubbels, comparison with equation 17

The high speed cinematography gives also information about the temporal decrease of the bubble diameter - which is closely related with the heat transfer at the phase interface. The duration of the bubble life can be expressed by the Fourier-number in a dimensionless form and using the experimental data the simple correlation

$$Fo = 1.784\ Re^{0.7}\ Pr^{0.5}\ Ja^{-1.0} \qquad (18)$$

for predicting the total condensation period was found. Up to a Jacob-number of 60 this equation corresponds well with measured data as figure 10 shows.

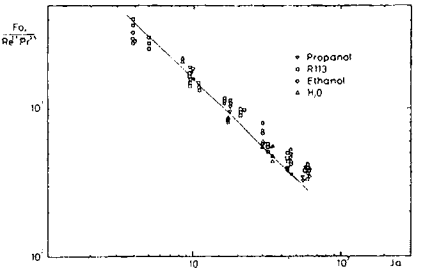

Fig.10: Condensation time,comparison of measured data and equation 18.

The temporal decrease of the bubble diameter can be predicted by using equation (19)

$$\beta = \left[1 - 0.56\ Re^{0.7}\ Pr^{0.5}\ Ja\ Fo\right]^{0.9} \qquad (19)$$

which was correlated from the data measured in this work.

5. CONCLUSIONS

The measurements with the holographic interferometry and the high speed cinematography showes that heat transfer and volumetric decrease of pure vapour bubbles condensing in a subcooled liquid of the same substance can be reliably correlated by using three dimensionless numbers namely the Jacob-, the Reynolds-, and the Prandtl-number. The Jacob-number gives a clear indication whether the heat transfer or the inertia is dominant in the condensing process. Up to Jacob-numbers of 60 - 80 the condensation is purely controlled by the heat transfer at the phase interface. After a situation of mixed conditions - heat transfer and inertia - with Jacob-numbers higher than 100 inertia forces then start to become the exclusive effect.

6. ACKNOWLEDGEMENT

The authors like to thank the Deutsche Forschungsgemeinschaft for the financial support of this work.

REFERENCES

1 Hammit,F.G.
Cavitation and multiphase flow phenomena
McGraw-Hill Inc. (1980)

2 Theofanous,T.G.;Biasi,L.;Isbin,H.S.;Fauske,H.K.
Non-equilibrium bubble collapse - a theoretical study
Chem.Eng.Prog.Symp.Ser.,Vol.66,102,37-47 (1970)

3 Plesset,M.S.
J.Appl.Mech.16,277-282 (1949)

4 Hammit,F.G.;Kling,C.L.
A photographic study of spark-induced cavitation bubble collapse
J.Basic Eng. 94,825-833 (1972)

5 Rayleigh,L.
On the pressure developed in a liquid during the collapse of a sperical cavity
Phil.Mag. 34,94-98 (1917)

6 Moalem,D.;Sideman,S.
The effect of motion on bubble collapse
Int.J.Heat Mass Transfer 16,2321-2329 (1973)

7 Akiyama,M.
Bubble collapse in subcooled boiling
Bulletin of the JSME 16,93,530-575 (1973)

8 Voloshko,A.A.;Vurgaft,A.V.;Aksel'rod,L.S.
Condensation of vapour bubbles in a liquid
Translated from Theoreticheski Osnovy Khimicheskoi,Tekhnologii,Vol.7,No.2,269-272 (1973)

9 Florschuetz,L.W.;Chao,B.T.
On the mechanics of vapour bubble collapse
J.Heat Transfer 87,209-220 (1965)

10 Voloshko,A.A.;Vurgaft,A.V.
Study of condensation of single vapour bubbles in a layer of subcooled liquid
Heat-Transfer-Soviet Research,Vol.3,No.2 (1971)

11 Dimić,M.
Collapse of one-component vapour bubbles with translatory motion
Int.J.Heat Mass Transfer 20,1322-1325 (1977)

12 Nordman,D.;Mayinger,F.
Temperatur ,Druck und Wärmetransport in der Umgebung kondensierender Blasen
VDI Forschungsheft Nr.605,S.3/36 (1981)